frontiers | Frontiers in Water

TYPE Original Research
PUBLISHED 29 August 2025
DOI 10.3389/frwa.2025.1636421

OPEN ACCESS

EDITED BY
Marcos D. Mateus,
Instituto Superior Técnico - Universidade de Lisboa, Portugal

REVIEWED BY
Sarah Praskievicz,
University of North Carolina at Greensboro, United States
Nicole Fernandez,
Cornell University, United States

*CORRESPONDENCE
Ricardo González-Pinzón
gonzaric@unm.edu

RECEIVED 27 May 2025
ACCEPTED 04 August 2025
PUBLISHED 29 August 2025

CITATION
Kaphle A, Rodríguez L, Tunby P, Nichols J, Khandelwal A, Joseph E, Aldred J, Van Horn DJ and González-Pinzón R (2025) Propagation of nutrients and metals after the 2022 Hermit's Peak-Calf Canyon gigafire. *Front. Water* 7:1636421. doi: 10.3389/frwa.2025.1636421

Propagation of nutrients and metals after the 2022 Hermit's Peak-Calf Canyon gigafire

Asmita Kaphle[1], Lina Rodríguez[1], Paige Tunby[1], Justin Nichols[1], Aashish Khandelwal[1], Eric Joseph[1], Jennifer Aldred[2], David J. Van Horn[3] and Ricardo González-Pinzón[1]*

[1]Department of Civil, Construction & Environmental Engineering, University of New Mexico, Albuquerque, NM, United States, [2]Natural Resources Management Department, New Mexico Highlands University, Las Vegas, NM, United States, [3]Department of Biology, University of New Mexico, Albuquerque, NM, United States

The increasing severity and frequency of wildfires in forested watersheds pose significant challenges to water quality management. This study examines the impacts of the 2022 Hermit's Peak-Calf Canyon gigafire, the largest wildfire in New Mexico's history. The wildfire burned over 1,382 km², affecting a key watershed that supplies drinking water to Las Vegas, NM. We conducted a longitudinal assessment of post-fire water quality dynamics across a 170 km fluvial network, analyzing flow, water quality parameters, nutrient and metal concentrations, and mobilization patterns. We found that post-fire nutrient concentrations exceeded pre-fire medians by up to two orders of magnitude. Our analyses revealed solute-specific transport patterns that are difficult to predict with static watershed- or fire-specific characteristics (e.g., burned area and percent severities). NH_4^+, PO_3^-, and NO_2^- were closely and positively associated with discharge and turbidity near the burn perimeter, while NO_3^- and TON exhibited strong mobilization trends ~170 km downstream. In contrast to nutrients, calcium, magnesium, and manganese levels showed no significant pre- vs. post-fire shifts, while concentrations of trace metals like Cr^{3+}, Pb^{2+}, Zn^{2+}, and Sr^{2+} surpassed background levels and public health thresholds. Our findings emphasize the significant propagation of wildfire disturbances over hundreds of kilometers and suggest the need for integrated watershed management strategies, including the management of large-scale flood control mechanisms to mitigate the far-reaching impacts of water quality disturbances post-fire.

KEYWORDS

wildfire, nutrients, metals, fluvial network, river corridor

Introduction

Forested watersheds provide critical ecosystem services, including water production, sediment filtration, and nutrient cycling, while serving as reservoirs for clean water storage and gradual release (Brauman et al., 2007; Leemans, 2009; Caldwell et al., 2023). In arid regions, these services are foundational to maintaining water quality and ecosystem health across large areas, as most precipitation falls in high elevation, forested mountains, which then supply arid downstream reaches with flow (Sharafatmandrad and Khosravi Mashizi, 2021; Li et al., 2022; Qiu et al., 2022). The functionality of forested watersheds in arid regions is being compromised by the increasing frequency and severity of wildfires (Bladon et al., 2014; Hohner et al., 2019; Ball et al., 2021). These terrestrial disturbances, driven by

climate change, prolonged droughts, and fire-suppression forest management practices, impact hydrological and biogeochemical processes, and reduce the capacity of watersheds to produce clean water (Adams, 2013; Abatzoglou and Williams, 2016; Emmerton et al., 2020).

Wildfire disturbances extend beyond burn scars and induce cascading effects along fluvial networks that stress watershed management operations (Reale et al., 2015; Ball et al., 2021; Nichols et al., 2024). First, wildfires induce hydrophobicity in soils when organic compounds from burning vegetation create a water-repellent layer (Giovannini et al., 1987; Huffman et al., 2001). This phenomenon reduces infiltration and increases runoff, facilitating the transport of sediments, nutrients, and contaminants into stream and river systems (Imeson et al., 1992; Johansen et al., 2001b; Gomez Isaza et al., 2022) including the mobilization of heavy metals, nitrates, and phosphates (Betts and Jones, 2009; Cerrato et al., 2016; Emelko et al., 2016; Rahman et al., 2018). These inputs can result in downstream ecological degradation by promoting harmful algal blooms, disrupting aquatic ecosystems, and creating public health risks (Robinne et al., 2018; Hohner et al., 2019; Tang et al., 2021; Olson et al., 2023). Besides generating impacts to natural ecosystems, the increased sediment transport post-fire typically exceeds the removal capacity of water treatment plants (Proctor et al., 2020; Elbein and Frazin, 2022), directly affecting downstream communities.

Despite the significant challenges brought by increased wildfire activity, there is a limited understanding of the spatiotemporal dynamics associated with the generation and propagation of wildfire disturbances (Ganteaume et al., 2021; Perera and Hong, 2023; Tampekis et al., 2023). Most research has focused on characterizing wildfire disturbances in areas near burn scars, leaving gaps in knowledge about their longitudinal propagation (Ball et al., 2021; Nichols et al., 2024). Understanding how these disturbances extend downstream is critical for resource management and restoration, to inform strategies to mitigate risks to water quality, protect ecosystem services, and to safeguard communities reliant on upstream forested watersheds (Robinne et al., 2021; Fraser et al., 2022; Paul et al., 2022; Belongia et al., 2023).

This study examines the impacts of the 2022 Hermits Peak-Calf Canyon gigafire, the largest wildfire in New Mexico's history, on the Gallinas Creek-Pecos River-Santa Rosa Lake fluvial network. The fire burned over 1,382 km^2 of forested areas, affecting 87% of a key watershed consistently used as the source of drinking water to the town of Las Vegas, NM (~13,000 inhabitants) (Khandelwal et al., 2023; Tunby et al., 2023; Nichols et al., 2024). Due to post-fire runoff events with sediment loads exceeding historical records by several orders of magnitude, the water treatment facility of Las Vegas, located about 30 km downstream of the headwaters of Gallinas Creek, had to close operations for 3 months, highlighting the susceptibility of coupled human-natural systems to wildfire disturbances. We deployed a rapid response research team to monitor key locations spanning 170 km to analyze water quality dynamics over a year post-fire. The goals of this study were to quantify the longitudinal impacts of wildfire disturbances on water quality parameters, nutrients, and metals, and identify opportunities to reduce exposure to disturbances at the watershed scale. Our data provide insights into key mobilization and dilution patterns over space and time, and evidence of how large-scale reservoirs can function as nutrient and sediment sinks, effectively attenuating the downstream propagation of wildfire disturbances.

Methods

Study area

The Hermit's Peak wildfire ignited on April 6, 2022, when a prescribed burn in the Santa Fe National Forest escalated out of control due to strong winds. Similarly, the Calf Canyon Fire, initially a dormant pile burn from January 2022, reignited and was declared a wildfire on April 19, 2022. These two fires merged on April 23, 2022, and expanded rapidly due to high winds, spreading to 600 km² within a month. By mid-June, the fire had grown to over 1,200 km², earning the designation of a gigafire (Linley et al., 2022). After burning a total of 1,382 km^2, this fire became the largest in New Mexico state recorded history. Seasonal monsoon rains helped slow the wildfire's progress, leading to full containment by August 21, 2022, nearly 5 months after it began. Our rapid response team examined the impact of this catastrophic event on the Gallinas Creek—Pecos River—Santa Rosa Lake fluvial network (Tunby et al., 2023).

Gallinas Creek, a tributary of the Pecos River, is the primary drinking water source for approximately 13,000 residents in Las Vegas, New Mexico. The Pecos River flows into Santa Rosa Lake, which is operated by the U.S. Army Corp of Engineers (USACE) for flood control, irrigation, recreation, and sediment retention. Our study included three sampling sites along the Gallinas Creek-Pecos River fluvial network, encompassing regions within the burn perimeter and extending ~170 km from the headwaters. These sites reflect a gradient of burned area impacts, land cover diversity, and anthropogenic influences, including drinking water intakes and wastewater treatment plant effluents. The first sampling site, GMZ, is situated within the burned area, 26 km downstream from the headwaters of Gallinas Creek, and receives input from a watershed that was 95.0% burned. The second site, GL, lies outside the burn perimeter, downstream of the town of Las Vegas, NM, and 61 km from the creek's headwaters. Its contributing watershed was 35.9% affected by the fire. The most downstream site, PSR, is located on the Pecos River, 167 km from the headwaters of Gallinas Creek, with 10.3% of its watershed area impacted by the fire. Site locations correspond to those in Nichols et al. (2024), with GMZ (P2), GL (P3), and PSR (P5). Sampling site and contributing watershed characteristics are summarized in Figure 1 and Supplementary Tables 1, 2.

Sampling and data collection

We recorded timeseries of water quality parameters, including turbidity, specific conductivity (SpCond), temperature, pH, dissolved oxygen (DO), and total dissolved solids (TDS) between April 2022 and September 2023 every 15 min using EXO2 water quality sondes at all three sites (GMZ, GL, and PSR). The time series data were corrected for outliers, sensor drifting, and biofouling using Aquarius Timeseries 21.1 (Aquatic Informatics, Vancouver,

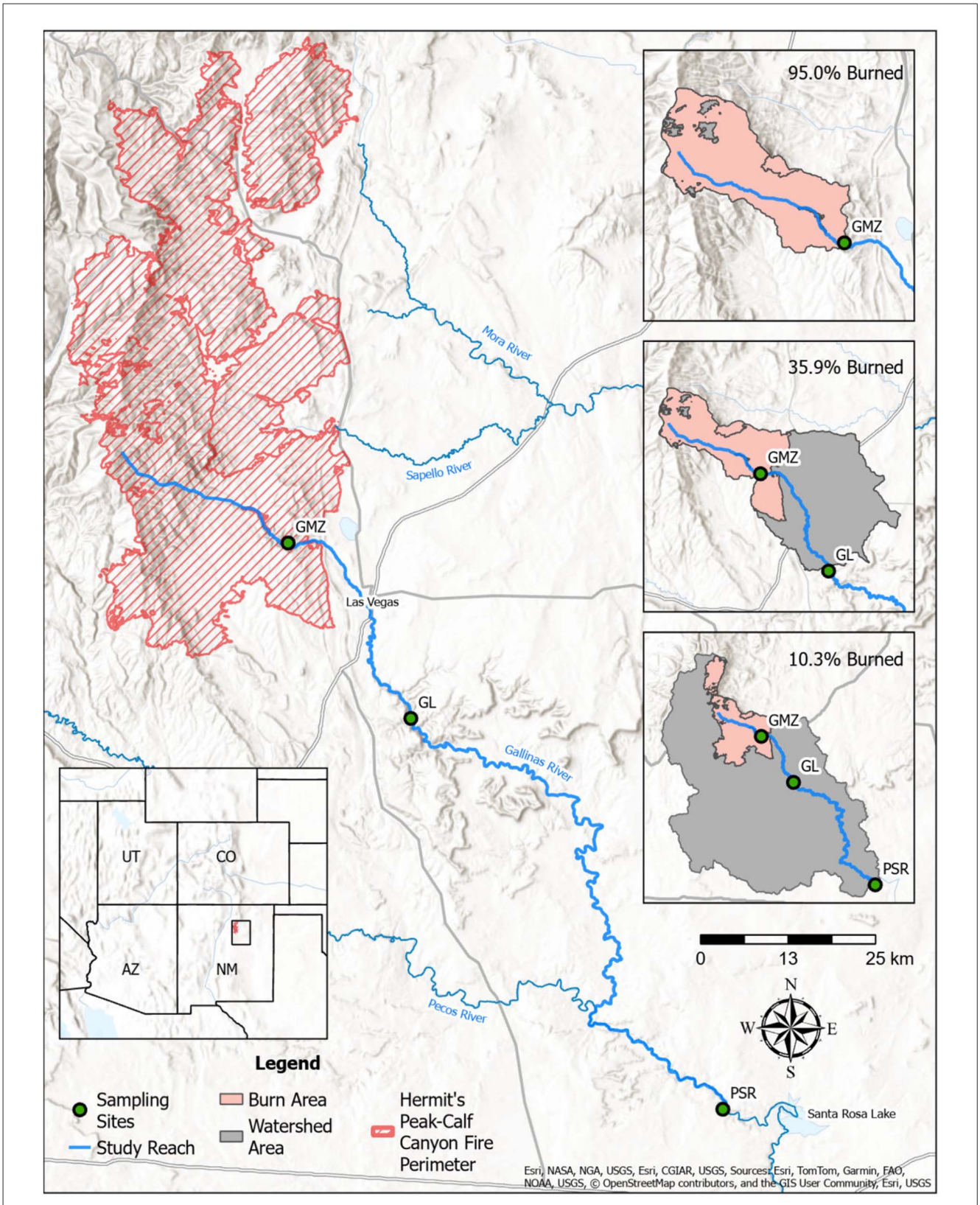

FIGURE 1
Map of grab sampling sites along the Gallinas-Pecos River-Santa Rosa fluvial network. Insets show catchment area maps of three contributing watersheds with orange portions denoting contributing burned areas. Sampling locations were labeled using names of the proximal stream gages, Gallinas Creek Near Montezuma (GMZ, site no 08380500), Gallinas River Near Lourdes (GL, site no 08382000), and Pecos River Above Santa Rosa Lake, NM (PSR, 08382650). Site locations correspond to those in Nichols et al. (2024), with GMZ (P2), GL (P3), and PSR (P5).

Canada). We read discharge data from co-located USGS stream gages (station nos. 08380500, 08382000, and 08382650).

We collected grab samples at the sensor sites for nutrient and metal analyses during sensor maintenance trips, i.e., every month, and during some post-fire storm events. Grab samples were filtered on-site using 0.45 µm nylon membranes and stored in pre-rinsed 20 mL polyethylene vials. Samples were immediately stored in a cooler during transport and frozen at −18 °C in the laboratory to prevent degradation. We collected 17, 24, and 8 viable grab samples from GMZ, GL, and PSR for nutrient analyses, and 10, 15, and 4 samples for metal analyses between Spring 2022 and 2023.

Historical discrete water quality data and pre-fire vs. post-fire comparisons

GMZ was the only site with historical water quality data available. There, the USGS New Mexico Water Science Center collected discrete samples for nutrients, metals, and sediments pre- and post-fire. Nitrate samples were collected between March 1964–June 1967 (16 samples, pre-fire) and July 2022-June 2023 (13 samples, post-fire). Phosphorus samples were collected between June 1987–October 1990 (13 samples, pre-fire) and July 2022–June 2023 (13 samples, post-fire). Sulfate samples were collected between March 1964–October 1990 (48 samples, pre-fire) and June 2022–June 2023 (14 samples, post-fire). Calcium values were available between July 1964-October 1990 (47 samples, pre-fire) and June 2023-June 2023 (14 samples, post-fire). Magnesium values were available between January 1965-October 1990 (44 samples, pre-fire) and June 2022-June 2023 (14 samples, post-fire). Manganese values were available between May 1988-May 1990 (5 samples, pre-fire) and between July 2022-October 2022 (2 samples, post-fire). Suspended sediment discharge (SSD, i.e., suspended sediment concentration (SSC) multiplied by discharge) values were available between June 1987-September 1990 (19 samples, pre-fire) and between June -September 2022 (10 samples, post-fire). Turbidity values were available between May 1988-September 1989 (10 samples, pre-fire) and June-October 2022 (10 samples, post-fire). Pre-fire turbidity data were reported in Jackson Turbidity Units (JTU) and post-fire data in nephelometric turbidity ratio units (NTRU). Both unit systems are roughly equivalent (Bash et al., 2001), and thus we used them interchangeably. Those data were retrieved from the online water monitoring report *How's My Waterway*, hosted by the Environmental Protection Agency (EPA). We used the non-parametric Mann-Whitney U statistical test to determine significant differences between pre- and post-fire discrete data since our populations had varying sizes.

Nutrient and metal concentrations

Thawed samples were analyzed for nitrate (NO_3^-), nitrite (NO_2^-), total oxidized nitrogen (TON), ammonium (NH_4^+), sulfate (SO_4^{2-}), and phosphate (PO_4^-) using a Thermo Fisher Gallery Discrete Analyzer. Analyses were based on EPA-approved colorimetric methods (U. S. Environmental Protection Agency, 1972a) and specific methods are detailed in Kaphle (2023).

Metals, including aluminum (Al^{3+}), calcium (Ca^{2+}), chromium (Cr^{3+}), magnesium (Mg^{2+}), manganese (Mn^{2+}), lead (Pb^{2+}), selenium (Se^{2-}), strontium (Sr^{2+}), and zinc (Zn^{2+}) were quantified using inductively coupled plasma optical emission spectroscopy (ICP-OES; PerkinElmer Optima 4300DV) (U. S. Environmental Protection Agency, 1972b); the specific methods are detailed in Kaphle (2023). Samples were acidified with 2% trace metal-grade nitric acid prior to analysis. Calibration and quality control procedures followed EPA guidelines (Lipps et al., 2023). Initial and continuing calibration verification (ICV and CCV) standards were used to ensure accuracy, with acceptance criteria of ±10%.

Sample concentrations below the limit of detection (LOD) were substituted with values of half LOD to provide reasonable statistical analyses (Lee and Helsel, 2005).

Data analysis

Concentration-discharge (C-Q) analysis

The C-Q relationships were modeled using the power-law Equation 1 (Hall, 1970, 1971; Chorover et al., 2017):

$$C = aQ^b\,, \tag{1}$$

where C is solute concentration, Q is discharge, a is the intercept, and b is the slope indicating mobilization ($b > 0$) or dilution ($b < 0$) trends. Export regimes were further characterized by the ratio of the coefficients of variation of C and Q (i.e., CV_c/CV_q). Chemostatic behavior is indicated when $CV_c/CV_q < 0.5$ and $-0.2 < b < 0.2$. Chemodynamic behavior occurs when $CV_c/CV_q > 0.5$ and $b > 0.2$ or $b < -0.2$ (Thompson et al., 2011; Musolff et al., 2015).

Mobilization conditions indicate that solute concentrations increase with discharge because solute sources become activated during high-flow conditions. Dilution conditions indicate that solute concentrations decrease with discharge, suggesting mixing with lower-concentration waters or storage effects. Both mobilization and dilution are classified as chemodynamic conditions. Chemostatic behavior indicates that concentrations remain stable, reflecting well-mixed or evenly distributed sources (Godsey et al., 2009; Musolff et al., 2015; Hohner et al., 2019; Knapp et al., 2020). C–Q relationships reflect integrated watershed responses, capturing the combined influences of source dynamics, flow paths, biogeochemical processes, and state factors (Wymore et al., 2019; Pohle et al., 2021).

Principal component analysis

We completed principal component analysis (PCA) to explore correlations among water quality parameters. PCA is a multivariate statistical method that reduces multiple variables into a smaller set of principal components that retain most of the original variability (Byrne et al., 2017). We standardized data using the Z-score normalization, which involves centering each variable by subtracting its mean and scaling by dividing by its standard deviation. This technique transforms all variables to a common

scale with a mean of zero and a standard deviation of one, removing differences in units and magnitudes. Data gaps were addressed using the "imputePCA" function from the missMDA package in R, which applies an iterative algorithm to estimate missing values. This method initially fills missing entries with the means of each variable, performs PCA, and iteratively refines the imputations using reconstruction formulas based on the principal components until convergence is reached (Josse and Husson, 2012). To ensure temporal consistency, daily averages of sensor and discharge data were calculated for the specific days on which grab samples were collected. Results were visualized through biplots showing parameter eigenvectors, where parameters aligned in the same direction represent positive correlations, those in opposite directions represent negative correlations, and those orthogonal are uncorrelated. PCAs were completed following Nichols et al. (2024).

Heatmap correlations

We conducted heatmap-based statistical comparisons to assess spatial differences in concentrations across monitoring sites. Pairwise Mann-Whitney U tests and *t*-tests were applied, with a Benjamini-Hochberg correction to control for multiple comparisons (Benjamini and Hochberg, 1995; Wilkinson and Friendly, 2009). We generated a *p*-value matrix, where heatmap colors indicated statistical significance at the threshold of $p < 0.05$ (Supplementary Information).

Results and discussion

Nutrients and water quality parameters

Pre-fire vs. post-fire changes in nutrients from historical records

From GMZ, the only station with pre-fire water quality data, we found significant ($p < 0.05$) differences between historical pre-fire and post-fire data for NO_3^-, total P, and $SO4^{2-}$ (Figure 2 and Supplementary Figure 1A). For NO_3^-, 19 and 92% of pre- and post-fire samples exceeded the pre-fire median value of 0.1 mg/L, respectively. The maximum NO_3^- concentrations exceeded the pre-fire median 4-fold and 43-fold pre- and post-fire, suggesting post-fire changes beyond typical seasonal variability. For total P, 46 and 100% of pre- and post-fire samples exceeded the pre-fire median value of 0.02 mg/L (as P), respectively. The maximum total P concentrations exceeded the pre-fire median 16-fold and 615-fold pre- and post-fire. In contrast, $SO4^{2-}$ showed a different trend, with decreasing concentrations after the fire. While 50% of pre-fire samples exceeded the median pre-fire level of 11.75 mg/L, only 21% of post-fire samples exceeded this mean. The lowest $SO4^{2-}$ concentrations were 2-fold and 3-fold lower than the pre-fire median pre- and post-fire, indicating a potential shift in its mobilization or dilution post-fire.

Despite the temporal limitations of the historical dataset, the observed patterns strongly suggest that the 2022 Hermit's Peak-Calf Canyon Fire triggered significant disturbances to nutrient transport in the watershed. While the pre-fire data do not capture more recent baseline variability, multiple lines of evidence support the validity of the comparison. The Gallinas Creek at Montezuma site has experienced minimal land use and land cover change over the monitoring period, remaining largely forested and protected as a drinking water source. In addition, discharge records indicate stable hydrological conditions since the 1920s, with no substantial long-term shifts attributable to climate variability. In Nichols et al. (2024), we showed that post-fire surface runoff increased relative to pre-fire conditions, with rainfall events typically common in the watershed (i.e., <2-year recurrence intervals) triggering unusually large runoff events, comparable to those expected only once every 10 years. In addition to these changes in runoff behavior, we showed that there were pronounced and prolonged alterations in daily water quality metrics and associated ecosystem processes that persisted for several months and were detectable at PSR. Nonetheless, we acknowledge that unmonitored factors such as gradual atmospheric deposition or long-term soil dynamics could contribute minor baseline shifts.

Post-fire variability of nutrients and correlations with water quality parameters and discharge

GMZ generally showed lower concentrations across most parameters (Supplementary Figure 2) and featured post-storm elevated values during Summer and Fall 2022. GL consistently exhibited the highest concentrations of NH_4^+, PO_4^{3-}, NO_2^-, NO_3^-, and TON, and still featured high post-storm values. This observation is relevant because while GMZ had 95% of its contributing area burned (Supplementary Table 2), GL only had 36%, suggesting that fire-related contributions are not easily scalable with watershed area or percentage of burned area, but that other near-site-specific factors pre-fire (i.e., watershed geomorphology, hill slopes) and post-fire (burn severity, precipitation volume and duration) can be significant factors driving nutrient export. PSR, the most downstream site where only 10% of the contributing watershed area was burned, showed substantial variability and elevated concentrations of SO_4^{2-}, NO_3^-, and TON, indicating cumulative effects of some nutrients. We found significant differences ($p < 0.05$) in all nutrient concentrations between GMZ and GL (Supplementary Figure 3) that suggest consistent increases in loading. However, GMZ and PSR sites were only different in SO_4^{2-} concentrations, highlighting GL as a key transition point for nutrient enrichment and suggesting a progressive stabilization of key nutrient concentrations along the fluvial network.

PCA biplots show that the first two principal components (PC1 and PC2) explained more than 69% of the total variance (Figure 3). At GMZ, NH_4^+, PO_4^{3-}, and NO_2^- are strongly positively correlated with both discharge and turbidity, indicating that these nutrients were mobilized during high-flow events and associated with sediment transport. This pattern was most evident in the Summer 2022 samples, which clustered in the direction of these vectors, suggesting elevated nutrient and turbidity levels during this period. In contrast, NO_3^- and TON aligned more with Spring 2023 samples and were not closely linked to discharge or turbidity, suggesting that they were more influenced by background sources, rather than storm-driven inputs. At GL, NH_4^+, NO_2^-, PO_4^{3-}, turbidity, and discharge were also tightly clustered and positively correlated, suggesting that high-flow conditions continue to drive nutrient

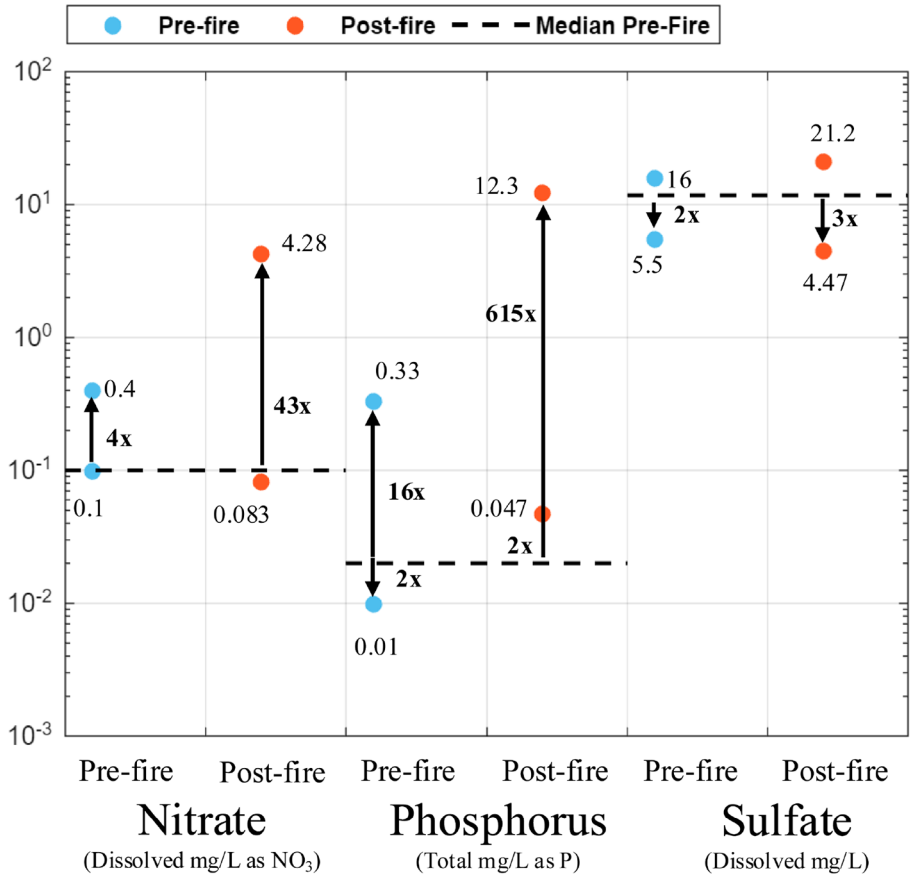

FIGURE 2
Comparison of pre-fire and post-fire concentrations of nitrate (NO_3^-), total phosphorus, and sulfate (SO_4^{2-}) at the GMZ sampling site. Blue and orange points represent pre-fire and post-fire extreme values, respectively, while the dashed black line indicates the pre-fire median concentration for each nutrient. Arrows indicate the magnitude of change in extreme concentrations relative to the pre-fire median, with fold increases or decreases greater than 2x labeled accordingly.

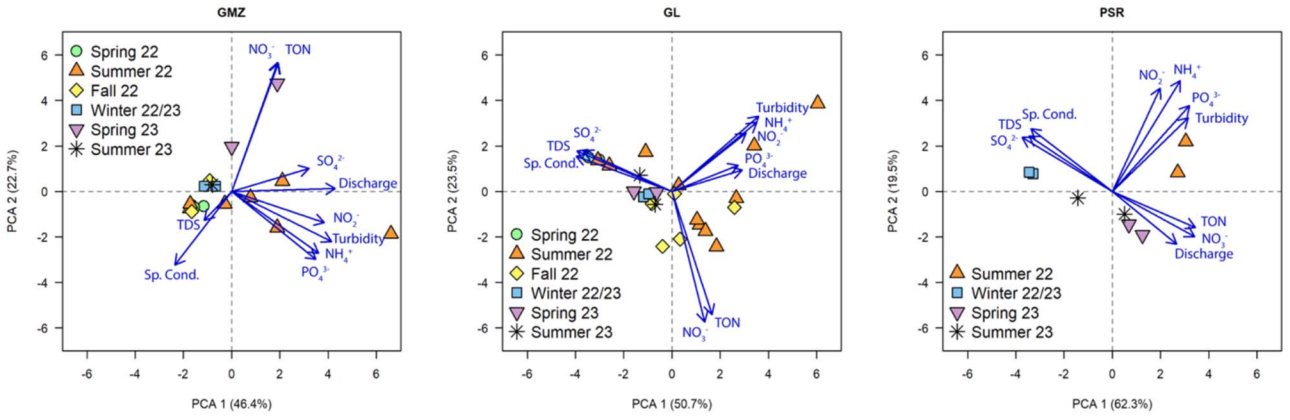

FIGURE 3
Principal component analysis (PCA) biplots illustrating site-specific correlations between water quality parameters (turbidity, specific conductivity termed as "Sp. Cond.", total dissolved solids termed as "TDS"), discharge, and concentrations of ammonium (NH_4^+), nitrate (NO_3^-), nitrite (NO_2^-), total oxidized nitrogen (TON), sulfate (SO_4^{2-}), and phosphate (PO_4^{3-}). Site locations correspond to those in Nichols et al. (2024), with GMZ (P2), GL (P3), and PSR (P5).

and sediment transport. Those variables align closely with Summer 2022 samples, highlighting elevated nutrient and turbidity levels during that season. In contrast, NO_3^- and TON were not associated with discharge or turbidity, suggesting that those nutrients were not driven by storm pulses, but remained high post-fire, as shown in the USGS data (Supplementary Figure 1) and our data (Figure 4).

Sp. Cond., SO_4^{2-}, and TDS vectors cluster together and point in an opposite direction, suggesting mineral-rich conditions are typical of baseflow periods, as seen in Spring 2022 and Winter 2022/23. At PSR, NH_4^+, PO_4^{3-}, NO_2^-, and turbidity clustered together, strongly influencing PC2, and were closely associated with the Summer 2022 samples, highlighting high nutrient concentrations and turbidity likely driven by storm events. NO_3^-, TON, and discharge strongly drove PC1 and aligned with Spring and Summer 2023 samples, suggesting nutrient enrichment tied to increased flow. Conversely, TDS, Sp. Cond., and SO_4^{2-} loaded heavily in the opposite direction, closely linked to Winter 2022/23, indicating their association with mineral-rich, low-flow base conditions and potential SO_4^{2-} reduction in anoxic zones.

Across the three sites, consistent patterns highlight spatial shifts in nutrient dynamics. At all sites, NH_4^+, PO_4^{3-}, and NO_2^- were strongly associated with turbidity and discharge, particularly during Summer 2022, suggesting event-driven nutrient pulses tied to surface runoff and sediment mobilization. However, downstream progression reveals increasing separation of nutrient vectors. At GMZ, NO_3^- and TON showed weaker links to discharge, while at PSR they aligned strongly with flow, indicating cumulative loading. In contrast, Sp. Cond., SO_4^{2-}, and TDS were most prominent during low-flow seasons (e.g., Winter 22/23) and were more influential upstream, suggesting stronger groundwater or geogenic signatures near the headwaters.

Export patterns of nutrients and water quality parameters

Concentration-discharge (C-Q) relationships provided insights into solute export regimes, distinguishing between mobilization, chemostatic, and dilution patterns. Figure 4 shows the C-Q relationships obtained for all water quality parameters and nutrients at each monitoring site and Supplementary Table 3 summarizes the results of the C-Q regressions obtained, where 15 out of 18 regressions were statistically significant. We observed positive C–Q slopes indicating mobilization at GMZ, GL and PSR for all N and P nutrients, but not for SO_4^{2-} at GL and PSR. The strongest nutrient responses to discharge happened at PSR, suggesting that multiple draining tributaries beyond Gallinas Creek (where GMZ and GL are located) actively drained nutrients post-storms to this remote site located ~170 km downstream of the burn perimeter. GMZ also displays mobilization behavior for nutrients like NO_3^- and TON, although it generally has slightly lower slopes than PSR, suggesting comparatively more limited wildfire-related contributions. In contrast, GL exhibited the most chemostatic behavior overall, with lower slopes across most nutrients, implying buffered or retentive responses.

NO_3^- and TON consistently showed the strongest mobilization patterns, with C–Q slopes (b) often exceeding 1 at GMZ and PSR, indicating greater increases in concentration than flow. This suggests substantial, readily mobilized sources of these nitrogen forms that are flushed post-fire. PO_4^{3-} exhibited moderate mobilization (C–Q slopes between 0.3 and 0.7), suggesting transport during flow events affected by soil sorption or biological uptake. In contrast, NH_4^+ showed near-chemostatic behavior with consistently low slopes across all sites, reflecting fast biological transformation, limited supply, or both (Godsey et al., 2009). NO_2^- featured variable behavior, showing stronger mobilization at GMZ and GL, with more chemostatic behavior at PSR, possibly due to uptake dynamics along the ~100 km GL-PSR reach. Finally, SO_4^{2-} was generally diluted at higher flows, with negative or near-zero C-Q slopes, especially at GL and PSR, suggesting minimal contributions from fire-related disturbances and sulfate reduction in anaerobic sediments.

Using the C-Q analysis based on coefficients of variation, we confirmed that PSR exhibited the strongest chemodynamic and mobilization behavior, particularly for NO_3^- and TON, indicating that flow events strongly influenced nutrient export. GMZ also showed mobilization trends but with less intensity, while GL featured a more chemostatic behavior (Figure 5). Overall, PSR exhibited the strongest mobilization dynamics for all nutrients, with an average C–Q slope (b) of 0.87 and the highest estimated mean CV_c/CV_q(~2.0), indicating both strong flow response and concentration variability. In contrast, GL had the lowest average slope (0.52) and the lowest CV_c/CV_q (~1.2). GMZ and PSR each had two nutrients (NO_3^- and TON) exhibiting strong mobilization ($b > 1$), but the slopes at PSR were higher. These differences suggest variability in hydrobiogeochemical responses across sites. Supplementary Table 4 includes the slope, intercept, and ratio of coefficients of variation for nutrient species.

Metals

Pre-fire vs. post-fire changes in metals from historical records

Our analysis of USGS data collected from the GMZ site suggested the lack of statistically significant differences ($p > 0.05$) in the concentrations of calcium (Ca^{2+}), magnesium (Mg^{2+}), and manganese (Mn^{2+}) between historical pre-fire and post-fire periods (Figure 6 and Supplementary Figure 1B). The pre-fire median concentration for Ca^{2+} was 44 mg/L, while the post-fire median was slightly lower at 37.3 mg/L. Neither the maximum nor the minimum Ca^{2+} concentrations deviated by more than twofold from the pre-fire median, aligning with the no-trend pattern reported by Paul et al. (2022), who found that for calcium and potassium, 77% of studies reported increases, 18% decreases, and 5% no trend. Mg^{2+} exhibited a similar pattern, with a pre-fire and post-fire median of 3.3 mg/L. Although the highest pre-fire concentrations of Mg^{2+} exceeded the median by sevenfold, post-fire maxima increased by less than twofold, indicating constrained variability. This result is consistent with other findings suggesting that some metal concentrations in post-fire runoff can remain relatively unchanged unless urban or highly disturbed landscapes are involved (Burke et al., 2013). Mn^{2+} showed the greatest variability among the three metals, but differences between pre- and post-fire values were not statistically significant. The pre-fire median concentration was 60 µg/L. Maximum concentrations exceeded the pre-fire median by twofold during the pre-fire period and by up to ninefold post-fire. Rhoades et al. (2019) noted that such short-term spikes are not uncommon and typically subside without long-term alteration of baseline metal levels. These results indicate that, unlike nutrients, the concentrations of these metals remained more stable following the 2022 Hermit's Peak-Calf Canyon Fire, likely due to rapid dilution or sedimentation of

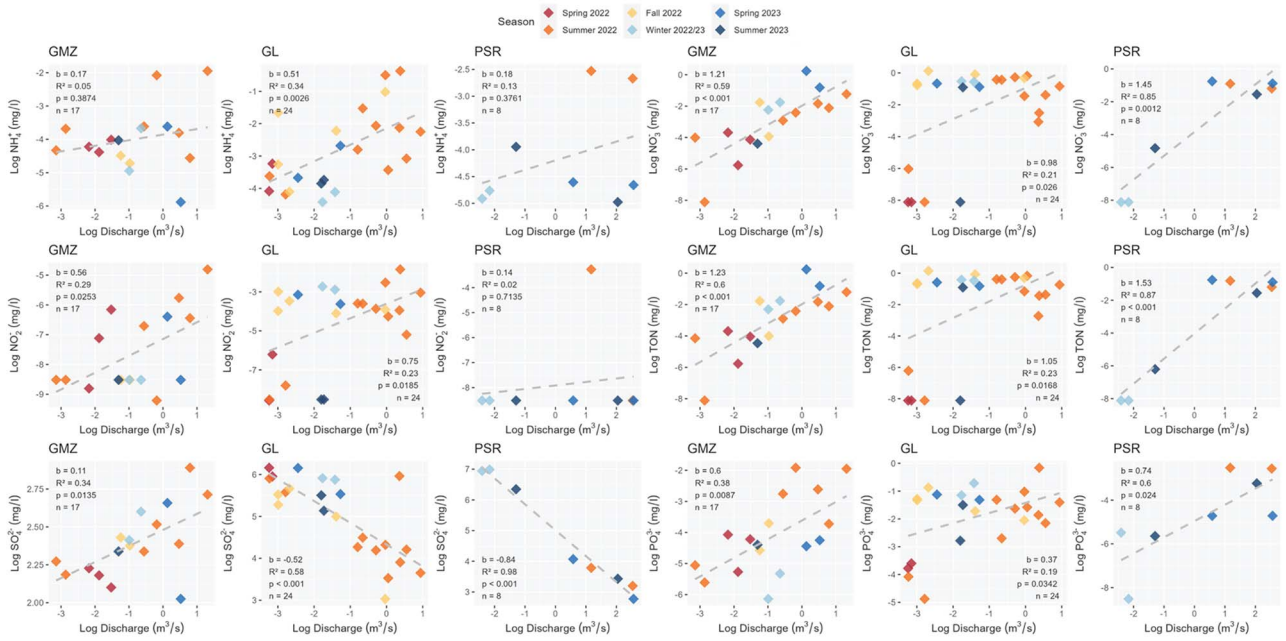

FIGURE 4
C-Q relationships of ammonium (NH_4^+), nitrate (NO_3^-), nitrite (NO_2^-), total oxidized nitrogen (TON), sulfate (SO_4^{2-}), and phosphate (PO_4^{3-}), with varying colors indicating samples taken during different seasons post-fire. Site locations correspond to those in Nichols et al. (2024), with GMZ (P2), GL (P3), and PSR (P5).

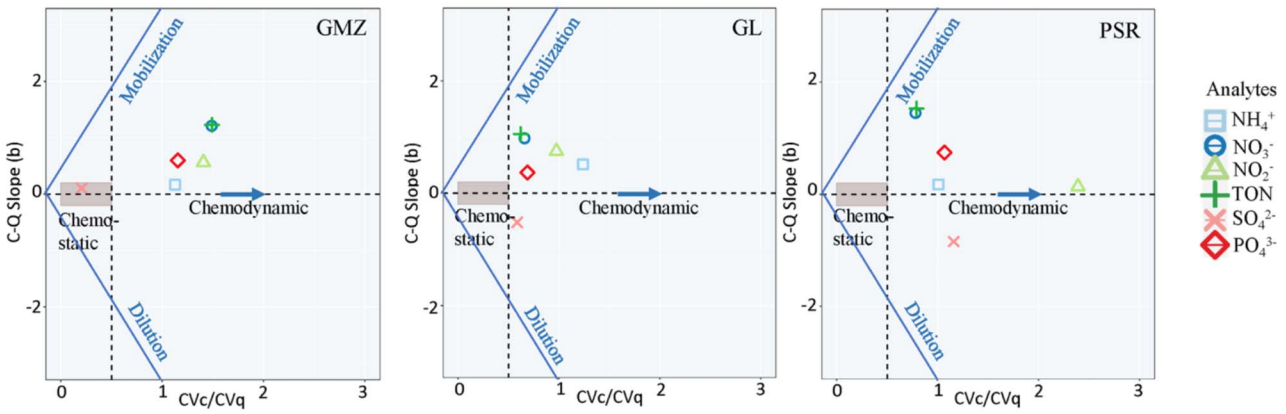

FIGURE 5
C-Q Slope (b) vs. CVc/CVq plot illustrating chemostatic and chemodynamic behavior of ammonium (NH_4^+), nitrate (NO_3^-), nitrite (NO_2^-), total oxidized nitrogen (TON), sulfate (SO_4^{2-}), and phosphate (PO_4^{3-}). Site locations correspond to those in Nichols et al. (2024), with GMZ (P2), GL (P3), and PSR (P5).

metal-bearing particles, and minimal anthropogenic or lithological metal sources in the immediate area.

Post-fire variability of metals

We captured differences in metal concentrations across sites. At GMZ, metal concentrations were moderately elevated across several elements but generally lower than those found further downstream at GL and PSR (Supplementary Figures 4,5). For example, Cr^{3+} concentrations at GMZ averaged ~0.04 mg/L, compared to ~0.06 mg/L at GL and ~0.09 mg/L at PSR. Similarly, Pb^{2+} at GMZ (~0.06 mg/L) was higher than the US EPA action level for drinking water supply of 0.010 mg/L (US EPA, 2015) but lower than at GL (~0.11 mg/L) and PSR (~0.12 mg/L), indicating a downstream increase in concentrations. Zn^{2+} showed a similar trend, with concentrations rising from ~0.06 mg/L at GMZ to ~0.08 mg/L at GL and spiking at ~0.30 mg/L at PSR. These concentrations are considerably higher than those typically observed in unaffected streams (~ 0.010 mg/L) (World Health Organization, 2003). Notably, GL exhibits a sharp increase in Ca^{2+} (~90 mg/L) and Mg^{2+} concentrations (~20 mg/L), likely influenced by local lithology or increased agricultural inputs, but these values may also reflect fire-enhanced weathering and ash

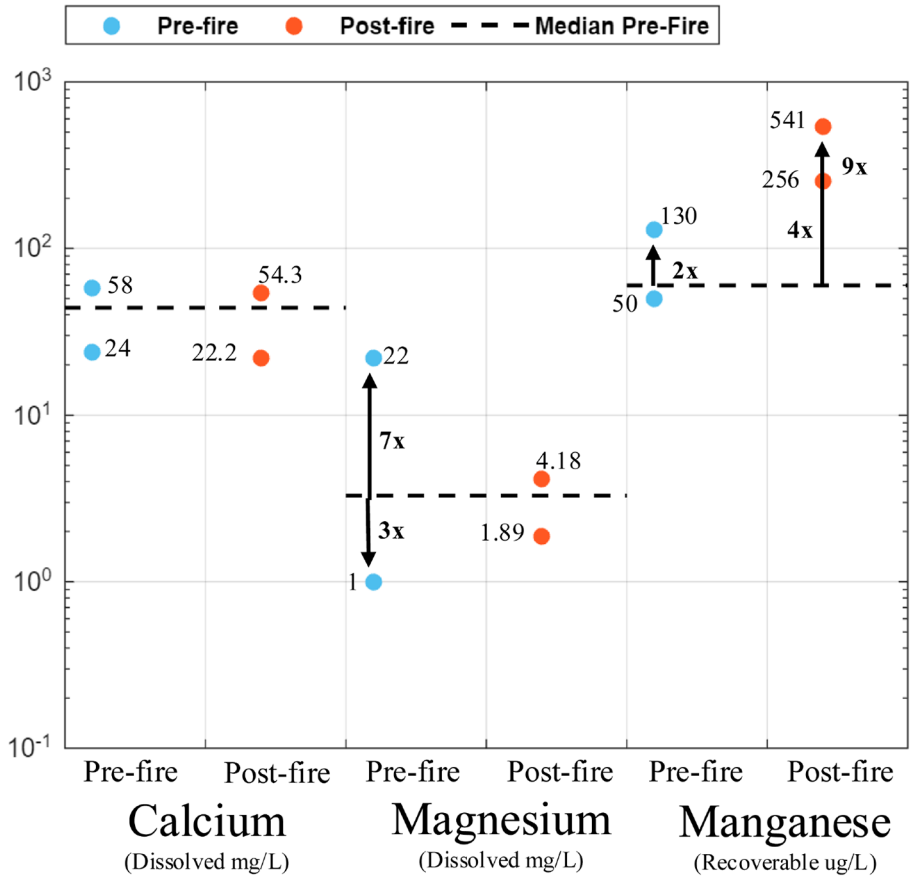

FIGURE 6
Comparison of pre-fire and post-fire concentrations of calcium (Ca^{2+}), magnesium (Mg^{2+}), and manganese (Mn^{2+}) at the GMZ sampling site. Blue and orange points represent pre-fire and post-fire extreme values, respectively, while the dashed black line indicates the pre-fire median concentration for each metal. Arrows indicate the magnitude of change in extreme concentrations relative to the pre-fire median, with fold increases or decreases greater than 2x labeled accordingly.

transport. Al^{3+} and Se^{2-} concentrations at GMZ and GL remained relatively low compared to more mobile metals like Pb^{2+} and Zn^{2+}, but both sites still recorded values exceeding typical natural background ranges and water quality international guidelines (Se^{2-} <0.04 mg/L) (World Health Organization, 2017). In both sites, concentrations of Mn^{2+} and Sr^{2+} were also higher than in most unburned reference systems (USGS, 1963), suggesting either fire-enhanced leaching or remobilization from disturbed soils.

We found elevated concentrations of Cr^{3+}, Pb^{2+}, Zn^{2+}, and Sr^{2+} at PSR. Cr^{3+} concentrations at this site (~0.05 mg/L) were more than double the typical background levels for unaffected streams (0.01–0.02 mg/L) and closely match concentrations in other post-fire studies (0.03–0.07 mg/L) (Smith et al., 2011). Similarly, Pb^{2+} levels at PSR (~0.12 mg/L) exceed natural background values (<0.05 mg/L) and align with ranges found in post-fire runoff (0.10–0.15 mg/L) (Gallaher and Koch, 2004). Zn^{2+} concentrations (~0.30 mg/L) also fall within the elevated post-fire range (0.25–0.35 mg/L), more than doubling the concentrations typically seen in unburned watersheds (~0.10 mg/L) (Johansen et al., 2001a). Sr^{2+} levels (~0.20 mg/L) at PSR are elevated relative to background (~0.10 mg/L) and are consistent with limited post-fire data showing increases up to 0.25 mg/L. These elevated concentrations suggest that wildfire effects can be transported long distances, driven by erosion, runoff from burned soils, and tributaries draining affected landscapes. Since we only captured 8 out of 27 C-Q regressions with statistical significance (p-value < 0.05), we do not focus our metal analysis on export patterns at a site or across sites, but make them available in Supplementary Figures 6–8.

Implications for water resource management

Our previous work on storm-runoff and longitudinal propagation analyses of water quality parameters showed that the wildfire disturbances generated from the 2022 Hermit's Peak-Calf Canyon Fire propagated to Santa Rosa Lake (Khandelwal et al., 2023; Nichols et al., 2024), which is located ~19 km downstream of PSR. Longitudinal monitoring along Santa Rosa Lake showed that water quality parameters changed due to sedimentation and lake circulation patterns (Khandelwal et al., 2023). In this study, we show that nutrients and metals generated from the fire

propagated ~170 km to PSR. This far-reaching propagation of post-fire water quality disturbances suggests the need to develop adaptive watershed management strategies that can help mitigate short- and large-scale spatiotemporal impacts.

The acute and chronic post-fire mobilization of sediments, nutrients, and metals propagating downstream of burn perimeters present significant risks for downstream water quality, with relevant implications for potable water supplies, agricultural irrigation, and aquatic ecosystem health (Rhoades et al., 2019; Proctor et al., 2020; Paul et al., 2022). Therefore, effective mitigation and remediation approaches to deal with wildfire impacts need to incorporate nested and integrated watershed-scale solutions. In response to the impacts of the 2022 Hermit's Peak–Calf Canyon wildfire, the U.S. Army Corps of Engineers (USACE) awarded a 7-million-dollar contract to implement rapid engineering solutions for protecting critical water infrastructure in the Gallinas Canyon from post-fire ash and debris transport (USACE-Albuquerque District Public Affairs, 2022). This initiative, part of the Gallinas Watershed Direct Assistance Project, was made possible through a contract action that allowed immediate construction (Supplementary Figure 9; USACE-Albuquerque District Public Affairs, 2022). The engineering structures implemented in the Gallinas Watershed after the Hermit's Peak–Calf Canyon wildfire were designed to cumulatively reduce the immediate post-fire impacts on critical water infrastructure (Supplementary Figure 10; Papaioannou et al., 2023; USACE-Albuquerque District Public Affairs, 2022). Gabion baskets, constructed of wire mesh filled with rocks, were deployed along stream banks and slopes to stabilize vulnerable areas and reduce erosion. Their porous design enables water to flow while filtering out larger debris, reducing erosion and sediment mobilization. Additionally, artificial log jams and other barriers were installed within stream channels to decelerate flows and promote sediment deposition. These structures can help to reduce the energy of incoming flows, minimizing the downstream transport of debris. The rapid deployment of these structures offered critical short-term protection, reducing immediate threats to water infrastructure (USACE-Albuquerque District Public Affairs, 2022).

Despite the timely work behind the installed post-fire mitigation and restoration strategies near the burn perimeter of the 2022 Hermit's Peak-Calf Canyon Fire, their impact on the longitudinal propagation of disturbances in the Gallinas Watershed appears to be limited since we continued to observe disturbances at GL and PSR that included higher nutrients, sediments, and even metals. Our work on longitudinal propagation of wildfire disturbances has shown that outside of high-steep regions, where natural flow and sediment transport regimes favor deposition, there are opportunities to design or use existing systems to prevent the mobilization of wildfire disturbances (Khandelwal et al., 2023; Tunby et al., 2023; Nichols et al., 2024). Our along-the-lake monitoring from Khandelwal et al. (2023) suggested that Santa Rosa Lake, a large-scale flood control reservoir, acted as a watershed-scale physical barrier that sank wildfire-related sediments and created biogeochemical reset points (e.g., turbidity decreased and dissolved oxygen increased), effectively mitigating the downstream propagation of disturbances by capturing peak volumes and concentrations associated with post-fire runoff events (Khandelwal et al., 2023). While localized interventions like the Gallinas Watershed Direct Assistance Project provided essential protection and immediate responses to proximal water quality concerns, the broader and more sustained impact of reservoirs highlights their critical role in dampening disturbances at the watershed scale. Reservoirs serve as control points by capturing the transport of sediments, nutrients, and organic materials, significantly moderating the downstream impacts of wildfire-related disruptions in river systems. Given their effectiveness, establishing dedicated flood control reservoirs within fire-prone areas could provide viable alternatives to help control far-reaching contamination of ecosystems through proactive and optimization-based management.

In arid regions, local, state, and federal agencies have already built large-scale reservoirs to manage the magnitude and timing of water resources (Kelly and Urbina, 2015) to protect the public from flooding and help meet complex water allocation rights (Fleck, 2016). Our findings suggest that those reservoirs can also be actively used to manage the episodic nature of wildfire disturbances, since they offer flow and sediment containment during peak runoff events thus serving as water quality buffers. Given the current increases in the frequency and extent of wildfires and associated impacts to fluvial networks (Ball et al., 2021), watershed managers should incorporate wildfire responses into the planned operational management of large-scale reservoirs to offer effective and longer-term solutions to communities affected by wildfires (U.S. Department of the Interior, 2024). We emphasize the active use of existing infrastructure first because building new large-scale projects requires extensive planning due to longer construction timelines, which are necessary to comply with regulatory standards, ensure structural safety, and address environmental concerns (Kelly and Urbina, 2015). However, new flood-control reservoirs could also provide a robust option to mitigate wildfire impacts in regions that are highly susceptible to recurrent wildfires.

Conclusions

The 2022 Hermit's Peak-Calf Canyon Fire caused severe water quality disturbances that persisted across the Gallinas-Pecos River-Santa Rosa Lake system for over a year. Our findings suggest that the fire significantly altered nutrient dynamics and, to a lesser extent, metal transport. We observed increases in nitrate, total phosphorus, and total oxidized nitrogen, particularly during high-flow events in the rainy season postfire (Summer 2022), indicating rapid nutrient mobilization linked to storm-driven surface runoff.

Near the burn perimeter, post-fire nutrient concentrations exceeded pre-fire medians by up to 615-fold for phosphorus and 43-fold for nitrate. Our analyses revealed distinct nutrient-specific transport patterns. NH_4^+, PO_4^-, and NO_2^- were closely associated with discharge and turbidity near the burn perimeter, while NO_3^- and TON exhibited stronger mobilization trends ~170 km downstream, suggesting cumulative nutrient loading and persistent post-fire sources. In contrast to nutrients, calcium, magnesium, and manganese levels showed no significant pre- vs. post-fire shifts, consistent with previous research indicating minimal fire effects on these metals in less urbanized or forested landscapes. However, concentrations of trace metals like Cr_3^-, Pb_2^+, Zn_2^+, and Sr_2^+ were elevated at downstream sites, surpassing

background levels and public health thresholds. Our results suggest site- and species-specific transport conditions that seem to contribute disproportionately to downstream nutrient and metal loads, indicating that watershed-scale responses are not strictly proportional to burned area or easily predictable from static fire-specific quantities such as burn severity or percentage of contributing watershed area burned.

Our findings emphasize the prolonged and spatially complex impacts of wildfire on watershed nutrient and metal dynamics. Post-fire nutrient mobilization can persist across seasons and propagate hundreds of kilometers downstream, requiring strategic water quality management, particularly during storm events. While localized mitigation measures, such as erosion control structures, can provide protection of critical infrastructure against large-scale debris near the burn perimeter, they do not prevent the widespread propagation of post-fire disturbances to distal sites.

Data availability statement

The datasets presented in this study can be found in online repositories. The names of the repository/repositories and accession number(s) can be found at: https://digitalrepository.unm.edu/ce_etds/319.

Author contributions

AsK: Validation, Conceptualization, Investigation, Supervision, Funding acquisition, Visualization, Resources, Data curation, Project administration, Formal analysis, Writing – review & editing, Methodology, Software, Writing – original draft. LR: Writing – review & editing, Writing – original draft, Formal analysis. PT: Writing – review & editing, Writing – original draft, Formal analysis. JN: Writing – review & editing, Writing – original draft, Methodology. AaK: Writing – original draft, Methodology, Writing – review & editing. EJ: Writing – review & editing, Writing – original draft, Methodology. JA: Writing – review & editing, Writing – original draft, Formal analysis. DV: Writing – review & editing, Formal analysis, Writing – original draft. RG-P: Data curation, Investigation, Supervision, Conceptualization, Writing – review & editing, Methodology, Software, Resources, Visualization, Project administration, Funding acquisition, Formal analysis, Validation, Writing – original draft.

Funding

The author(s) declare that financial support was received for the research and/or publication of this article. The National Science Foundation funded this work through grants CBET 2054444 to RG-P and DV, and HDR 1914490 to RG-P. USACE supported part of this research through Cooperative Agreement W912HZ-14-2-0014. The New Mexico Water Resources Research Institute also funded part of this research through faculty and student grants to RG-P and Asmita K.

Acknowledgments

We thank Lea Knutson and Conrad Greaves from the Hermit's Peak Watershed Alliance for helping us secure site access to monitoring stations.

Conflict of interest

The authors declare that the research was conducted in the absence of any commercial or financial relationships that could be construed as a potential conflict of interest.

Generative AI statement

The author(s) declare that no Gen AI was used in the creation of this manuscript.

Any alternative text (alt text) provided alongside figures in this article has been generated by Frontiers with the support of artificial intelligence and reasonable efforts have been made to ensure accuracy, including review by the authors wherever possible. If you identify any issues, please contact us.

Publisher's note

All claims expressed in this article are solely those of the authors and do not necessarily represent those of their affiliated organizations, or those of the publisher, the editors and the reviewers. Any product that may be evaluated in this article, or claim that may be made by its manufacturer, is not guaranteed or endorsed by the publisher.

Supplementary material

The Supplementary Material for this article can be found online at: https://www.frontiersin.org/articles/10.3389/frwa.2025.1636421/full#supplementary-material

References

Abatzoglou, J. T., and Williams, A. P. (2016). Impact of anthropogenic climate change on wildfire across western US forests. *Proc. Natl. Acad. Sci. U.S.A.* 113, 11770–11775. doi: 10.1073/pnas.1607171113

Adams, M. A. (2013). Mega-fires, tipping points and ecosystem services: managing forests and woodlands in an uncertain future. *For. Ecol. Manage.* 294, 250–261. doi: 10.1016/j.foreco.2012.11.039

Ball, G., Regier, P., González-Pinzón, R., Reale, J., and Van Horn, D. (2021). Wildfires increasingly impact western US fluvial networks. *Nat. Commun.* 12:2484. doi: 10.1038/s41467-021-22747-3

Bash, J., Berman, C., and Bolton, S. (2001). *Effects of Turbidity and Suspended Solids on Salmonids*. University of Washington Water Center. Available online at: https://digital.lib.washington.edu/researchworks/items/91e9fb0c-e579-48f2-a897-813416c0faa1

Belongia, M. F., Hammond Wagner, C., Seipp, K. Q., and Ajami, N. K. (2023). Building water resilience in the face of cascading wildfire risks. *Sci. Adv*. 9:eadf9534. doi: 10.1126/sciadv.adf9534

Benjamini, Y., and Hochberg, Y. (1995). Controlling the false discovery rate: a practical and powerful approach to multiple testing. *J. R. Stat. Soc. Ser. B.* 57, 289–300. doi: 10.1111/j.2517-6161.1995.tb02031.x

Betts, E. F., and Jones, J. B. (2009). Impact of wildfire on stream nutrient chemistry and ecosystem metabolism in boreal forest catchments of interior Alaska. *Arct. Antarct. Alp. Res.* 41, 407–417. doi: 10.1657/1938-4246-41.4.407

Bladon, K. D., Emelko, M. B., Silins, U., and Stone, M. (2014). Wildfire and the future of water supply. *Environ. Sci. Technol.* 48, 8936–8943. doi: 10.1021/es500130g

Brauman, K. A., Daily, G. C., Duarte, T. K., and Mooney, H. A. (2007). The nature and value of ecosystem services: an overview highlighting hydrologic services. *Annu. Rev. Environ. Resour.* 32, 67–98. doi: 10.1146/annurev.energy.32.031306.102758

Burke, M. P., Hogue, T. S., Kinoshita, A. M., Barco, J., Wessel, C., Stein, E. D., et al. (2013). Pre- and post-fire pollutant loads in an urban fringe watershed in Southern California. *Environ. Monit. Assess* 185, 10131–10145. doi: 10.1007/s10661-013-3318-9

Byrne, P., Runkel, R. L., and Walton-Day, K. (2017). Synoptic sampling and principal components analysis to identify sources of water and metals to an acid mine drainage stream. *Environ. Sci. Pollut. Res.* 24, 17220–17240. doi: 10.1007/s11356-017-9038-x

Caldwell, P. V., Martin, K. L., Vose, J. M., Baker, J. S., Warziniack, T. W., Costanza, J. K., et al. (2023). Forested watersheds provide the highest water quality among all land cover types, but the benefit of this ecosystem service depends on landscape context. *Sci. Total Environ.* 882:163550. doi: 10.1016/j.scitotenv.2023.163550

Cerrato, J. M., Blake, J. M., Hirani, C., Clark, A. L., Ali, A-. M. S., Artyushkova, K., et al. (2016). Wildfires and water chemistry: effect of metals associated with wood ash. *Environ. Sci. Processes Impacts* 18, 1078–1089. doi: 10.1039/C6EM00123H

Chorover, J., Derry, L. A., and McDowell, W. H. (2017). Concentration-discharge relations in the critical zone: implications for resolving critical zone structure, function, and evolution. *Water Resour. Res.* 53, 8654–8659. doi: 10.1002/2017WR021111

Elbein, S., and Frazin, R. (2022). *DRIED UP: Compounding Fires and Floods in Southwest Pose Dire Threat to Drinking Water*. The Hill. Available online at: https://thehill.com/policy/equilibrium-sustainability/3686361-dried-up-compounding-fires-and-floods-in-southwest-pose-dire-threat-to-drinking-water/

Emelko, M. B., Stone, M., Silins, U., Allin, D., Collins, A. L., Williams, C. H. S., et al. (2016). Sediment-phosphorus dynamics can shift aquatic ecology and cause downstream legacy effects after wildfire in large river systems. *Glob. Chang Biol.* 22, 1168–1184. doi: 10.1111/gcb.13073

Emmerton, C. A., Cooke, C. A., Hustins, S., Silins, U., Emelko, M. B., Lewis, T., et al. (2020). Severe western Canadian wildfire affects water quality even at large basin scales. *Water Res.* 183:116071. doi: 10.1016/j.watres.2020.116071

Fleck, J. (2016). *Water is for Fighting Over: And Other Myths about Water in the West*. Washington, DC: Island Press.

Fraser, A. M., Chester, M. V., and Underwood, B. S. (2022). Wildfire risk, post-fire debris flows, and transportation infrastructure vulnerability. *Sustain. Resilient Infrastruct.* 7, 188–200. doi: 10.1080/23789689.2020.1737785

Gallaher, B. M., and Koch, R. J. (2004). *Cerro Grande Fire Impact to Water Quality and Stream Flow near Los Alamos National Laboratory: Results of Four Years of Monitoring*. Los Alamos, NM (US): Los Alamos National Lab. doi: 10.2172/835908

Ganteaume, A., Barbero, R., Jappiot, M., and Maillé, E. (2021). Understanding future changes to fires in southern Europe and their impacts on the wildland-urban interface. *J. Saf. Sci. Resilience* 2, 20–29. doi: 10.1016/j.jnlssr.2021.01.001

Giovannini, G., Lucchesi, S., and Giachetti, M. (1987). The natural evolution of a burned soil: a three-year investigation. *Soil Sci.* 143, 220–226. doi: 10.1097/00010694-198703000-00009

Godsey, S. E., Kirchner, J. W., and Clow, D. W. (2009). Concentration-discharge relationships reflect chemostatic characteristics of US catchments. *Hydrol. Process.* 23, 1844–1864. doi: 10.1002/hyp.7315

Gomez Isaza, D. F., Cramp, R. L., and Franklin, C. E. (2022). Fire and rain: a systematic review of the impacts of wildfire and associated runoff on aquatic fauna. *Global Change Biol.* 28, 2578–2595. doi: 10.1111/gcb.16088

Hall, F. R. (1970). Dissolved solids-discharge relationships: 1. Mixing models. *Water Resour. Res.* 6, 845–850. doi: 10.1029/WR006i003p00845

Hall, F. R. (1971). Dissolved solids-discharge relationships: 2. Applications to field data. *Water Resour. Res.* 7, 591–601. doi: 10.1029/WR007i003p00591

Hohner, A. K., Rhoades, C. C., Wilkerson, P., and Rosario-Ortiz, F. L. (2019). Wildfires alter forest watersheds and threaten drinking water quality. *Acc. Chem. Res.* 52, 1234–1244. doi: 10.1021/acs.accounts.8b00670

Huffman, E. L., MacDonald, L. H., and Stednick, J. D. (2001). Strength and persistence of fire-induced soil hydrophobicity under ponderosa and lodgepole pine, Colorado Front Range. *Hydrol. Process.* 15, 2877–2892. doi: 10.1002/hyp.379

Imeson, A. C., Verstraten, J. M., van Mulligen, E. J., and Sevink, J. (1992). The effects of fire and water repellency on infiltration and runoff under Mediterranean type forest. *CATENA* 19, 345–361. doi: 10.1016/0341-8162(92)90008-Y

Johansen, M., Enz, B., Gallaher, B., Mullen, K., and Kraig, D. (2001a). *Storm Water Quality in Los Alamos Canyon following the Cerro Grande Fire*. Los Alamos, NM (United States): Los Alamos National Lab. (LANL).

Johansen, M. P., Hakonson, T. E., and Breshears, D. D. (2001b). Post-fire runoff and erosion from rainfall simulation: contrasting forests with shrublands and grasslands. *Hydrol. Process.* 15, 2953–2965. doi: 10.1002/hyp.384

Josse, J., and Husson, F. (2012). Handling missing values in exploratory multivariate data analysis methods. *J. Soc. Franç. Statist.* 153, 79–99. Available online at: https://www.numdam.org/item/JSFS_2012__153_2_79_0/

Kaphle, A. (2023). *Post-Wildfire Export Regimes Of Solutes Along The Gallinas-Pecos River-Santa Rosa Fluvial Network*. Available online at: https://digitalrepository.unm.edu/ce_etds/319

Kelly, S., and Urbina, D. (2015). New Mexico's major reservoirs: an overview. *Water Matters* 1, 20-1-20-18. Available online at: https://digitalrepository.unm.edu/utton_watermatters/vol2015/iss1/25

Khandelwal, A., Castillo, T., and González-Pinzón, R. (2023). Development of the navigator: a Lagrangian sensing system to characterize surface freshwater ecosystems. *Water Res.* 245:120577. doi: 10.1016/j.watres.2023.120577

Knapp, J. L. A., Von Freyberg, J., Studer, B., Kiewiet, L., and Kirchner, J. W. (2020). Concentration-discharge relationships vary among hydrological events, reflecting differences in event characteristics. *Hydrol. Earth Syst. Sci.* 24, 2561–2576. doi: 10.5194/hess-24-2561-2020

Lee, L., and Helsel, D. (2005). Statistical analysis of water-quality data containing multiple detection limits: S-language software for regression on order statistics. *Comp. Geosci.* 31, 1241–1248. doi: 10.1016/j.cageo.2005.03.012

Leemans, R. (2009). "The millennium ecosystem assessment: securing interactions between ecosystems, ecosystem services and human well-being," in *Hexagon Series on Human and Environmental Security and Peace* (Springer: Berlin, Heidelberg), 53–61. doi: 10.1007/978-3-540-68488-6_3

Li, Y., Liu, W., Feng, Q., Zhu, M., Yang, L., Zhang, J., et al. (2022). Quantitative assessment for the spatiotemporal changes of ecosystem services, tradeoff-synergy relationships and drivers in the semi-arid regions of China. *Remote Sens.* 14:239. doi: 10.3390/rs14010239

Linley, G. D., Jolly, C. J., Doherty, T. S., Geary, W. L., Armenteras, D., Belcher, C. M., et al. (2022). What do you mean, 'megafire'? *Global Ecol. Biogeogr.* 31, 1906–1922. doi: 10.1111/geb.13499

Lipps, W. C., Braun-Howland, E. B., Baxter, T. E., American Public Health Association, American Water Works Association, and Water Environment Federation eds. (2023). *Standard Methods for the Examination of Water and Wastewater, 24th Edn*. Washington: American Public Health Association.

Musolff, A., Schmidt, C., Selle, B., and Fleckenstein, J. H. (2015). Catchment controls on solute export. *Adv. Water Resour.* 86, 133–146. doi: 10.1016/j.advwatres.2015.09.026

Nichols, J., Joseph, E., Kaphle, A., Tunby, P., Rodriguez, L., Khandelwal, A., et al. (2024). Longitudinal propagation of aquatic disturbances following the largest wildfire recorded in New Mexico, USA. *Nat. Commun.* 15:7143. doi: 10.1038/s41467-024-51306-9

Olson, N. E., Boaggio, K. L., Rice, R. B., Foley, K. M., and LeDuc, S. D. (2023). Wildfires in the western United States are mobilizing PM2.5-associated nutrients and may be contributing to downwind cyanobacteria blooms. *Environ. Sci. Processes Impacts* 25, 1049–1066. doi: 10.1039/D3EM00042G

Papaioannou, G., Alamanos, A., and Maris, F. (2023). Evaluating post-fire erosion and flood protection techniques: a narrative review of applications. *GeoHazards* 4, 380–405. doi: 10.3390/geohazards4040022

Paul, M. J., LeDuc, S. D., Lassiter, M. G., Moorhead, L. C., Noyes, P. D., and Leibowitz, S. G. (2022). Wildfire induces changes in receiving waters: a review with considerations for water quality management. *Water Resour. Res.* 58:e2021WR030699. doi: 10.1029/2021WR030699

Perera, A. T. D., and Hong, T. (2023). Vulnerability and resilience of urban energy ecosystems to extreme climate events: a systematic review and perspectives. *Renewable Sustain. Energy Rev.* 173:113038. doi: 10.1016/j.rser.2022.113038

Pohle, I., Baggaley, N., Palarea-Albaladejo, J., Stutter, M., and Glendell, M. (2021). A framework for assessing concentration-discharge catchment behavior from low-frequency water quality data. *Water Resour. Res.* 57:e2021WR029692. doi: 10.1029/2021WR029692

Proctor, C. R., Lee, J., Yu, D., Shah, A. D., and Whelton, A. J. (2020). Wildfire caused widespread drinking water distribution network contamination. *AWWA Water Sci.* 2:e1183. doi: 10.1002/aws2.1183

Qiu, J., Huang, T., and Yu, D. (2022). Evaluation and optimization of ecosystem services under different land use scenarios in a semiarid landscape mosaic. *Ecol. Indic.* 135:108516. doi: 10.1016/j.ecolind.2021.108516

Rahman, A., El Hayek, E., Blake, J. M., Bixby, R. J., Ali, A-. M., Spilde, M., et al. (2018). Metal reactivity in laboratory burned wood from a watershed affected by wildfires. *Environ. Sci. Technol.* 52, 8115–8123. doi: 10.1021/acs.est.8b00530

Reale, J. K., Van Horn, D. J., Condon, K. E., and Dahm, C. N. (2015). The effects of catastrophic wildfire on water quality along a river continuum. *Freshwater Sci.* 34, 1426–1442. doi: 10.1086/684001

Rhoades, C. C., Nunes, J. P., Silins, U., and Doerr, S. H. (2019). The influence of wildfire on water quality and watershed processes: new insights and remaining challenges. *Int. J. Wildland Fire* 28:721. doi: 10.1071/WFv28n10_FO

Robinne, F. N., Bladon, K. D., Miller, C., Parisien, M. A., Mathieu, J., Flannigan, M. D., et al. (2018). A spatial evaluation of global wildfire-water risks to human and natural systems. *Sci. Total Environ.* 610–611, 1193–1206. doi: 10.1016/j.scitotenv.2017.08.112

Robinne, F-. N., Hallema, D. W., Bladon, K. D., Flannigan, M. D., Boisramé, G., Bréthaut, C. M., et al. (2021). Scientists' warning on extreme wildfire risks to water supply. *Hydrol. Process.* 35:e14086. doi: 10.1002/hyp.14086

Sharafatmandrad, M., and Khosravi Mashizi, A. (2021). Temporal and spatial assessment of supply and demand of the water-yield ecosystem service for water scarcity management in arid to semi-arid ecosystems. *Water Resour. Manage.* 35, 63–82. doi: 10.1007/s11269-020-02706-1

Smith, H. G., Sheridan, G. J., Lane, P. N. J., Nyman, P., and Haydon, S. (2011). Wildfire effects on water quality in forest catchments: a review with implications for water supply. *J. Hydrol.* 396, 170–192. doi: 10.1016/j.jhydrol.2010.10.043

Tampekis, S., Sakellariou, S., Palaiologou, P., Arabatzis, G., Kantartzis, A., Malesios, C., et al. (2023). Building wildland-urban interface zone resilience through performance-based wildfire engineering. A holistic theoretical framework. *Euro-Mediterr. J. Environ. Integr.* 8, 675–689. doi: 10.1007/s41207-023-00385-z

Tang, W., Llort, J., Weis, J., Perron, M. M. G., Basart, S., Li, Z., et al. (2021). Widespread phytoplankton blooms triggered by 2019–2020 Australian wildfires. *Nature* 597, 370–375. doi: 10.1038/s41586-021-03805-8

Thompson, S. E., Basu, N. B., Lascurain, J., Aubeneau, A., and Rao, P. S. C. (2011). Relative dominance of hydrologic versus biogeochemical factors on solute export across impact gradients. *Water Resour. Res.* 47:WR009605. doi: 10.1029/2010WR009605

Tunby, P., Nichols, J., Kaphle, A., Khandelwal, A. S., Van Horn, D. J., González-Pinzón, R., et al. (2023). Development of a general protocol for rapid response research on water quality disturbances and its application for monitoring the largest wildfire recorded in New Mexico, USA. *Front. Water* 5:1223338. doi: 10.3389/frwa.2023.1223338

U.S. Department of the Interior (2024). *Biden-Harris Administration Announces $35 Million from Investing in America Agenda for Small Storage Projects in California and Utah*. U.S. Department of the Interior. Available online at: https://www.doi.gov/pressreleases/biden-harris-administration-announces-35-million-investing-america-agenda-small

US EPA, O. (2015). *National Primary Drinking Water Regulations*. US EPA.

USACE-Albuquerque District Public Affairs (2022). *Contract Awarded, Construction Started in Gallinas Watershed.* US Army Corps of Engineers. Available online at: https://www.spa.usace.army.mil/Media/News-Releases/Article/3064677/contract-awarded-construction-started-in-gallinas-watershed/#:~:text=ALBUQUERQUE%2C%20N.M.%20%E2%80%93%20The%20U.S.%20Army,caused%20by%20the%20local%20wildfires

U. S. Environmental Protection Agency. (1972a). *Approved CWA Test Methods: Inorganic Non-Metals*. U. S. Environmental Protection Agency.

U. S. Environmental Protection Agency. (1972b). *Approved CWA Test Methods: Metals*. U. S. Environmental Protection Agency.

USGS (1963). *Occurrence and Distribution of Strontium in Natural Water*. USGS.

Wilkinson, L., and Friendly, M. (2009). The history of the cluster heat map. *Am. Stat.* 63, 179–184. doi: 10.1198/tas.2009.0033

World Health Organization (2003). *Zinc in Drinking-Water: Background Document for Preparation of WHO Guidelines for Drinking-Water Quality*. Geneva: World Health Organization.

World Health Organization (2017). *Guidelines for Drinking-Water Quality: Fourth Edition Incorporating First Addendum, 4th Edn, 1st add.* Geneva: World Health Organization.

Wymore, A. S., Leon, M. C., Shanley, J. B., and McDowell, W. H. (2019). Hysteretic response of solutes and turbidity at the event scale across forested tropical montane watersheds. *Front. Earth Sci.* 7:126. doi: 10.3389/feart.2019.00126